# A Class of Frequency-Domain Adaptive Approaches to Blind Multichannel Identification

Yiteng (Arden) Huang, *Member, IEEE,* and Jacob Benesty, *Member, IEEE*

***Abstract*—In this paper, we extend our previous studies on adaptive blind channel identification from the time domain into the frequency domain. A class of frequency-domain adaptive approaches, including the multichannel frequency-domain LMS (MCFLMS) and constrained/unconstrained normalized multichannel frequency-domain LMS (NMCFLMS) algorithms, are proposed. By utilizing the fast Fourier transform (FFT) and overlap-save techniques, the convolution and correlation operations that are computationally intensive when performed by the time-domain multichannel LMS (MCLMS) or multichannel Newton (MCN) methods are efficiently implemented in the frequency domain, and the MCFLMS is rigorously derived. In order to achieve independent and uniform convergence for each filter coefficient and, therefore, accelerate the overall convergence, the coefficient updates are properly normalized at each iteration, and the NMCFLMS algorithms are developed. Simulations show that the frequency-domain adaptive approaches perform as well as or better than their time-domain counterparts and the cross-relation (CR) batch method in most practical cases. It is remarkable that for a three-channel acoustic system with long impulse responses (256 taps in each channel) excited by a male speech signal, only the proposed NMCFLMS algorithm succeeds in determining a reasonably accurate channel estimate, which is good enough for applications such as time delay estimation.**

***Index Terms*—Blind channel identification, frequency-domain adaptive filtering, least mean square, multichannel signal processing.**

## I. Introduction

SYSTEM identification is the technique of building a mathematical model of an unknown dynamic system by analyzing its input/output data. This problem of fundamental interest arises in a variety of signal processing and communications applications. The ability to identify a system facilitates a better understanding of how an input signal is transmitted/processed/distorted by the system and, therefore, enables a practical attempt to equalize the dispersive effect introduced by the fading channels and/or to design a more efficient communications system. Since, in practice, the system is generally nonstationary and usually has a long impulse response, determining its characteristics is not easy, even when the input signal is known *a priori*, such as in the case of acoustic echo cancellation. However, in many other cases, e.g., acoustic dereverberation, wireless communications, time delay estimation, etc., the input is either unobservable or very expensive to acquire; the choice inevitably comes down to a blind method, and as a result, the channels are more difficult to estimate.

The innovative idea of blind channel identification and equalization was first proposed by Sato in [1]. Since then, many algorithms have been proposed. Broadly, one can dichotomize these approaches into the class of second-order statistics (SOS) methods and the class of higher order statistics (HOS) methods. Because HOS cannot be accurately computed from a small number of observations, slow convergence is the critical drawback of all existing HOS methods. In addition, a cost function based on the HOS is barely concave, and an HOS algorithm can be misled to a local minimum by corrupting noise in the observations. Since it was recognized that the problem can be solved in the light of only SOS [2], the focus of the blind channel identification research has shifted to SOS methods, behind which, the motivation is the potential for fast convergence. There is a rich literature on SOS blind channel identification. Many batch methods have had good success to some extent, such as the subspace (SS) algorithm [3], the cross relation (CR) algorithm [4], [5], the least squares component normalization (LSCN) algorithm [6], the linear prediction based subspace (LP-SS) algorithm [7], and the two-step maximum likelihood (TSML) algorithm [8] (see [9] for a review on the SOS methods and the references therein).

According to [10], a satisfactory blind channel identification algorithm needs to satisfy three design requirements:

1) quick convergence;
2) adaptivity;
3) low complexity.

Most SOS batch methods can converge quickly, but unfortunately, they are difficult to implement in an adaptive mode [9] and are in general computationally intensive. In an earlier study [11], we developed an adaptive eigenvalue decomposition algorithm to blindly identify a single-input two-output acoustic FIR system for time delay estimation in reverberant environments. The idea was later used by Berberidis *et al.* for channel equalization in communications [12]. Even though the generalization of the adaptive algorithm from a two-channel to a multichannel system seems straightforward, its derivation is not easy since the algebraic complexity increases dramatically with the number of channels. In [13], an error signal based on the cross relations between different channels was constructed in a systematic way for a single-input multiple-output (SIMO) FIR system, and the corresponding cost function was concise. As a result, the use of adaptive filtering techniques is potentially facilitated in determining the desired channel impulse responses. A multichannel LMS (MCLMS) algorithm and a multichannel Newton (MCN) method were proposed. Their convergence in the mean to the real channel impulse responses was theoretically shown and empirically justified by numerical studies. However, none of these

Manuscript received November 7, 2001; revised August 19, 2002. The associate editor coordinating the review of this paper and approving it for publication was Dr. Inbar Fijalkow.

The authors are with Bell Laboratories, Lucent Technologies, Murray Hill, NJ 07974 USA (e-mail: arden@research.bell-labs.com; jbenesty@bell-labs.com).

Digital Object Identifier 10.1109/TSP.2002.806559

time-domain adaptive algorithms is perfect. The MCLMS algorithm converges slowly though steadily, and the MCN method needs to invert a nondiagonal Hessian matrix, which involves extensive computation.

Time-frequency analysis utilizing the fast Fourier transform (FFT) is an important mathematical tool in signal processing. Since its first introduction by Dentino *et al.* [14], adaptive filtering in the frequency-domain has attracted a great deal of research interest and recently has become an essential constituent of adaptive filtering theory. By taking advantage of the computational efficiency of the FFT, a convolution of two signals can be quickly calculated. Moreover, a discrete Fourier transform (DFT) processes a time sequence like a filterbank, which orthogonalizes the data, and therefore, the coefficients of a frequency-domain adaptive filter can converge independently or even uniformly if the update is normalized properly. For single-channel cases, the derivation and implementation of a frequency-domain adaptive filter is rather simple. However, when multiple channels are considered, the algorithmic complexity increases significantly with the number of channels.

In this paper, we extend our study of the blind multichannel identification problem in the frequency domain and aim to achieve an improved efficient adaptive filter. We propose a whole class of multichannel adaptive filtering algorithms in the frequency domain. A multichannel frequency-domain LMS (MCFLMS) algorithm is first proposed, and its derivation is rigorous. Then, both constrained and nonconstrained normalized multichannel frequency-domain LMS (NMCFLMS) algorithms are developed with a clear discussion on what approximations are made. In order to evaluate these proposed algorithms, several practical numerical experiments are conducted. Both random sequence and speech signals are used as the source to excite the system. In terms of the channel, we investigate randomly generated short impulse responses and long impulse responses created by the image model [15]. For the latter, none of the existing blind channel identification algorithms, to the best of our knowledge, succeeds even when the signal-to-noise ratio (SNR) is high, but the proposed NMCFLMS algorithm shows the ability to identify a speech-driven system with reasonable accuracy. This intriguing and inspiring result lets the NMCFLMS algorithm find direct applications in speech processing.

## II. Problem Formulation and Background

### A. Notation

Before formulating the addressed problem and developing the proposed algorithm, we define the notation used in this paper, which is mostly standard in the time domain, but is specifically defined in the frequency domain. Uppercase and lowercase bold letters denote time-domain matrices and vectors, respectively. In the frequency domain, matrices and vectors are represented, respectively, by uppercase calligraphic and lowercase bold *italic* letters, and a vector is further emphasized by an underbar. The difference in their appearance is illustrated by the following example:

- $\mathbf{x}$ vector in the time domain (bold, lowercase);
- $\mathbf{X}$ matrix in the time domain (bold, uppercase);
- $\underline{\boldsymbol{x}}$ vector in the frequency domain (bold italic, lowercase, with an underbar);
- $\boldsymbol{\mathcal{X}}$ matrix in the frequency domain (calligraphic, uppercase).

Following standard convention, the operators $E\{\cdot\}$, $(\cdot)^*$, $(\cdot)^T$, and $(\cdot)^H$ stand for mathematical expectation, complex conjugate, vector/matrix transpose, and Hermitian transpose, respectively. The symbols $*$, $\otimes$, $\odot$, and $\nabla$ denote, respectively, linear convolution, circular convolution, the Schur (element-by-element) product, and the gradient operator. The identity matrix is given by $\mathbf{I}$, whose dimension is either implied by the context or explicitly specified by a subscript.

### B. Channel Model and Identifiability

Consider a single-input multiple-output (SIMO) FIR linear system, as shown in Fig. 1. The $i$th channel output signal $x_i(n)$ is the result of a linear convolution between the source signal $s(n)$ and the corresponding channel impulse response $h_i$, corrupted by an additive background noise $b_i(n)$:

$$x_i(n) = h_i * s(n) + b_i(n), \; i = 1, 2, \ldots, M \tag{1}$$

where $M$ is the number of channels. In vector form, (1) can be expressed as

$$\mathbf{x}_i(n) = \mathbf{H}_i \cdot \mathbf{s}(n) + \mathbf{b}_i(n) \tag{2}$$

where we have the equation at the bottom of the page, and $L$ is set to the length of the longest channel impulse response by assumption. The channel parameter matrix $\mathbf{H}_i$ is of dimension $L \times (2L-1)$ and is constructed from the channel's impulse response

$$\mathbf{h}_i = [\,h_{i,0} \quad h_{i,1} \quad \cdots \quad h_{i,L-1}\,]^T. \tag{3}$$

Moreover, the additive noise components in different channels are assumed to be uncorrelated with the source signal, even though they might be mutually dependent.

A blind channel identification algorithm is to estimate the channel impulse responses $\mathbf{h}_i$ ($i = 1, 2, \ldots, M$) from the ob-

$$\mathbf{x}_i(n) = [\,x_i(n) \quad x_i(n-1) \quad \cdots \quad x_i(n-L+1)\,]^T$$

$$\mathbf{H}_i = \begin{bmatrix} h_{i,0} & h_{i,1} & \cdots & h_{i,L-1} & 0 & \cdots & 0 \\ 0 & h_{i,0} & \cdots & h_{i,L-2} & h_{i,L-1} & \cdots & 0 \\ \vdots & \ddots & \ddots & \vdots & \ddots & \ddots & \vdots \\ 0 & \cdots & 0 & h_{i,0} & h_{i,1} & \cdots & h_{i,L-1} \end{bmatrix}$$

$$\mathbf{s}(n) = [\,s(n) \quad s(n-1) \quad \cdots \quad s(n-L+1) \quad \cdots \quad s(n-2L+2)\,]^T$$

$$\mathbf{b}_i(n) = [\,b_i(n) \quad b_i(n-1) \quad \cdots \quad b_i(n-L+1)\,]^T$$

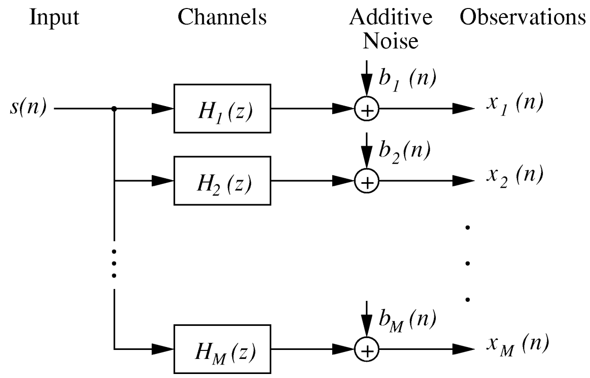


Fig. 1. Illustration of the relationships between the input $s(n)$ and the observations $x_i(n)$ in a single-input multiple-output FIR system.

servations $\mathbf{x}_i$ without utilizing the source signal $\mathbf{s}(n)$. The following two assumptions (one on the channel diversity and the other on the input source signal) are made throughout this paper to guarantee an identifiable system [5].

1) The polynomials formed from $\mathbf{h}_i,\ i = 1, 2, \ldots M$, are co-prime, i.e., the channel transfer functions $H_i(z)$ do not share any common zeros.
2) The autocorrelation matrix $\mathbf{R}_{ss} = E\left\{\mathbf{s}(n)\mathbf{s}^T(n)\right\}$ of the source signal is of full rank.

### *C. Fundamentals and Adaptive Time-Domain Approaches*

The channel impulse responses of an identifiable system can be blindly determined using only the second-order statistics of channel outputs since the vector of channel impulse responses lies in the null space of the cross-correlation like matrix $\mathbf{R}$ of channel outputs [6]

$$\mathbf{R}\mathbf{h} = \mathbf{0} \tag{4}$$

where

$$\mathbf{R} = \begin{bmatrix} \sum_{i\neq 1}\mathbf{R}_{x_ix_i} & -\mathbf{R}_{x_2x_1} & \cdots & -\mathbf{R}_{x_Mx_1} \\ -\mathbf{R}_{x_1x_2} & \sum_{i\neq 2}\mathbf{R}_{x_ix_i} & \cdots & -\mathbf{R}_{x_Mx_2} \\ \vdots & \vdots & \ddots & \vdots \\ -\mathbf{R}_{x_1x_M} & -\mathbf{R}_{x_2x_M} & \cdots & \sum_{i\neq M}\mathbf{R}_{x_ix_i} \end{bmatrix}$$

$$\mathbf{R}_{x_ix_j} = E\left\{\mathbf{x}_i(n)\mathbf{x}_j^T(n)\right\},\ i,j = 1,2,\ldots,M$$
$$\mathbf{h} = \left[\mathbf{h}_1^T \quad \mathbf{h}_2^T \quad \cdots \quad \mathbf{h}_M^T\right]^T.$$

The adaptive multichannel LMS (MCLMS) and multichannel Newton (MCN) algorithms proposed in [13] approach the desired solution by minimizing an error criterion based on the cross-relation between the channel outputs. By following the fact that

$$x_i * h_j = s * h_i * h_j = x_j * h_i,\ i,j = 1,2,\ldots,M,\ i \neq j \tag{5}$$

we have, in the absence of noise, the following relation at time $n$:

$$\mathbf{x}_i^T(n)\mathbf{h}_j = \mathbf{x}_j^T(n)\mathbf{h}_i,\ i,j = 1,2,\ldots,M,\ i \neq j. \tag{6}$$

When noise is present, the cross-relation (5) fails and an error signal is defined:

$$e_{ij}(n) = \begin{cases} \mathbf{x}_i^T(n)\mathbf{h}_j - \mathbf{x}_j^T(n)\mathbf{h}_i, & i \neq j,\ i,j = 1,2,\ldots,M \\ 0, & i = j,\ i,j = 1,2,\ldots,M. \end{cases} \tag{7}$$

In order to avoid the trivial estimate of all zero elements, a unit-norm constraint is imposed on $\mathbf{h}$, and the normalized error signal becomes

$$\begin{aligned} \epsilon_{ij}(n) &= \begin{cases} \frac{\mathbf{x}_i^T(n)\mathbf{h}_j}{\|\mathbf{h}\|} - \frac{\mathbf{x}_j^T(n)\mathbf{h}_i}{\|\mathbf{h}\|}, & i \neq j,\ i,j = 1,2,\ldots,M \\ 0, & i = j,\ i,j = 1,2,\ldots,M \end{cases} \\ &= \frac{e_{ij}(n)}{\|\mathbf{h}\|}. \end{aligned} \tag{8}$$

Accordingly, the cost function is specified as

$$J(n) = \sum_{i=1}^{M-1}\sum_{j=i+1}^{M}\epsilon_{ij}^2(n) \tag{9}$$

and the estimate of the channel impulse responses is given by

$$\hat{\mathbf{h}} = \arg\min_{\mathbf{h}} E\{J(n)\},\ \text{ subject to } \left\|\hat{\mathbf{h}}\right\| = 1. \tag{10}$$

The channel estimate of the MCLMS algorithm [13] is updated adaptively as

$$\hat{\mathbf{h}}(n+1) = \frac{\hat{\mathbf{h}}(n) - 2\mu\left[\tilde{\mathbf{R}}(n)\hat{\mathbf{h}}(n) - J(n)\hat{\mathbf{h}}(n)\right]}{\left\|\hat{\mathbf{h}}(n) - 2\mu\left[\tilde{\mathbf{R}}(n)\hat{\mathbf{h}}(n) - J(n)\hat{\mathbf{h}}(n)\right]\right\|} \tag{11}$$

where $\mu$ is a small positive step size and where we have the equation at the bottom of the page. It was shown in [13] that the MCLMS is able to converge in the mean to the desired solution, which is the eigenvector of $\mathbf{R}$ corresponding to the smallest eigenvalue $E\{J(\infty)\}$. Furthermore, the convergence can be accelerated, still in the time domain, by using Newton's method.

$$\tilde{\mathbf{R}}(n) = \begin{bmatrix} \sum_{i\neq 1}\tilde{\mathbf{R}}_{x_ix_i}(n) & -\tilde{\mathbf{R}}_{x_2x_1}(n) & \cdots & -\tilde{\mathbf{R}}_{x_Mx_1}(n) \\ -\tilde{\mathbf{R}}_{x_1x_2}(n) & \sum_{i\neq 2}\tilde{\mathbf{R}}_{x_ix_i}(n) & \cdots & -\tilde{\mathbf{R}}_{x_Mx_2}(n) \\ \vdots & \vdots & \ddots & \vdots \\ -\tilde{\mathbf{R}}_{x_1x_M}(n) & -\tilde{\mathbf{R}}_{x_2x_M}(n) & \cdots & \sum_{i\neq M}\tilde{\mathbf{R}}_{x_ix_i}(n) \end{bmatrix}$$

$$\tilde{\mathbf{R}}_{x_ix_j}(n) = \mathbf{x}_i(n)\mathbf{x}_j^T(n),\ i,j = 1,2,\ldots,M.$$

## III. Multichannel Frequency-Domain LMS Algorithm

The time-domain MCLMS and MCN algorithms exploit the channel diversity and minimize an error criterion in a novel and systematic way, which leads to algebraic simplicity. Their ability to adapt makes it possible to apply blind multichannel identification techniques in many practical applications. However, the MCLMS algorithm converges slowly, and the MCN method is computationally intensive since it needs to determine the inverse of a nondiagonal Hessian matrix. Neither of these algorithms is satisfactory for a real-time system. We intend to improve the technique and propose several frequency-domain approaches in the following two sections. Although a block delay will be unavoidably introduced in a frequency-domain implementation, such a delay is tolerable for most applications.

### A. Algorithm Derivation

In order to determine the error signal in (7), we need to calculate the convolution of the $i$th channel output $x_i$ $(i = 1, 2, \ldots, M)$ and the impulse response $\hat{h}_j$ $(j = 1, 2, \ldots, M)$ of the $j$th model filter. As illustrated in Fig. 2, we let $y_{ij} \triangleq x_i * \hat{h}_j$ denote such a convolution result. When $L$ and $M$ are large, these convolutions are computationally intensive in the time domain. Therefore, we intend to perform digital filtering efficiently in the frequency domain as follows.

The frequency-domain LMS (FLMS) algorithm is based on the overlap-save technique [16] used for frequency-domain filtering. In matrix notation, the vector $\tilde{\mathbf{y}}_{ij}(m)$ $(i, j = 1, 2, \ldots, M)$ of length $2L$ that results from the *circular convolution* of $\mathbf{x}_i$ and $\hat{\mathbf{h}}_j$ is given by

$$\tilde{\mathbf{y}}_{ij}(m) = \mathbf{C}_{x_i} \hat{\mathbf{h}}_j^{10}(m) \tag{12}$$

where $m$ is the block time index and where we have the first equation at the bottom of the page. Note that $\mathbf{C}_{x_i}(m)$ is a circulant matrix. We can see from inspection that the last $L$ points

其實 last $L+1$ 都 identical

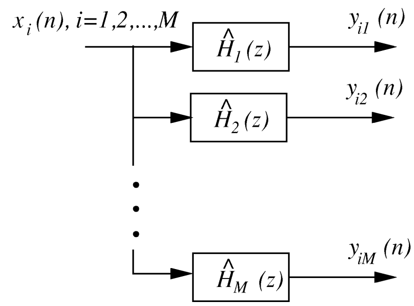


Fig. 2. Block diagram illustrating the signals $y_{ij}, i, j = 1, 2, \ldots, M$ defined in the derivation of the multichannel frequency-domain adaptive algorithms for blind channel identification.

in the output, i.e., $\tilde{y}_{ij}(mL), \ldots, \tilde{y}_{ij}(mL + L - 1)$ are identical to the results of a linear convolution

$$\begin{aligned} \mathbf{y}_{ij}(m) =& \mathbf{W}_{L\times 2L}^{01} \tilde{\mathbf{y}}_{ij}(m) = \mathbf{W}_{L\times 2L}^{01} \mathbf{C}_{x_i} \hat{\mathbf{h}}_j^{10}(m) \\ =& \mathbf{W}_{L\times 2L}^{01} \mathbf{C}_{x_i} \mathbf{W}_{2L\times L}^{10} \hat{\mathbf{h}}_j(m) \end{aligned} \tag{13}$$

where we have the second equation at the bottom of the page. Utilizing the overlap-save technique, the input data blocks are overlapped by $L$ points. For each block of length $L$, where we have $2L$ data inputs, discard the first $L$ circular convolution results, and retain only the last $L$ results as outputs.

As such, a block of the error signal based on the cross-relation between the $i$th and the $j$th channel is determined as

$$\begin{aligned} \mathbf{e}_{ij}(m) =& \mathbf{y}_{ij}(m) - \mathbf{y}_{ji}(m) \\ =& \mathbf{W}_{L\times 2L}^{01} \Big[ \mathbf{C}_{x_i} \mathbf{W}_{2L\times L}^{10} \hat{\mathbf{h}}_j(m) - \mathbf{C}_{x_j} \mathbf{W}_{2L\times L}^{10} \hat{\mathbf{h}}_i(m) \Big]. \end{aligned} \tag{14}$$

Next, we use the FFT technique to efficiently perform a circular convolution. Let $\mathbf{F}_{L\times L}$ be the Fourier matrix of size $L \times L$, whose element at $(p, q)$ is given by

$$(\mathbf{F}_{L\times L})_{p,q} = e^{-j2\pi pq/L}, \; p, q = 0, 1, \ldots, L-1. \tag{15}$$

---

$$\tilde{\mathbf{y}}_{ij}(m) = [\tilde{y}_{ij}(mL - L) \quad \tilde{y}_{ij}(mL - L + 1) \quad \cdots \quad \tilde{y}_{ij}(mL) \quad \cdots \quad \tilde{y}_{ij}(mL + L - 1)]^T$$

$$\mathbf{C}_{x_i}(m) = \begin{bmatrix} x_i(mL - L) & x_i(mL + L - 1) & \cdots & x_i(mL - L + 1) \\ x_i(mL - L + 1) & x_i(mL - L) & \cdots & x_i(mL - L + 2) \\ \vdots & \vdots & \ddots & \vdots \\ x_i(mL) & x_i(mL - 1) & \cdots & x_i(mL + 1) \\ \vdots & \vdots & \ddots & \vdots \\ x_i(mL + L - 1) & x_i(mL + L - 2) & \cdots & x_i(mL - L) \end{bmatrix}$$

$$\hat{\mathbf{h}}_j^{10}(m) = [\hat{\mathbf{h}}_j^T(m) \quad \mathbf{0}_{L\times 1}^T]^T = [\hat{h}_{j,0}(m) \quad \hat{h}_{j,1}(m) \quad \cdots \quad \hat{h}_{j,L-1}(m) \quad 0 \quad \cdots \quad 0]^T.$$

---

$$\begin{aligned} \mathbf{y}_{ij}(m) &= [y_{ij}(mL) \quad y_{ij}(mL + 1) \quad \cdots \quad y_{ij}(mL + L - 1)]^T \\ \mathbf{W}_{L\times 2L}^{01} &= [\mathbf{0}_{L\times L} \quad \mathbf{I}_{L\times L}] \\ \mathbf{W}_{2L\times L}^{10} &= [\mathbf{I}_{L\times L} \quad \mathbf{0}_{L\times L}]^T \\ \hat{\mathbf{h}}_j(m) &= [\hat{h}_{j,0}(m) \quad \hat{h}_{j,1}(m) \quad \cdots \quad \hat{h}_{j,L-1}(m)]^T. \end{aligned}$$

Then, the relationship between $\mathbf{F}_{L\times L}$ and its inverse $\mathbf{F}_{L\times L}^{-1}$ is found as

$$\mathbf{F}_{L\times L}^{H} = L\mathbf{F}_{L\times L}^{-1}. \tag{16}$$

By utilizing $\mathbf{F}_{2L\times 2L}$ and $\mathbf{F}_{2L\times 2L}^{-1}$, a circulant matrix can be decomposed as

$$\mathbf{C}_{x_i}(m) = \mathbf{F}_{2L\times 2L}^{-1}\boldsymbol{\mathcal{D}}_{x_i}(m)\mathbf{F}_{2L\times 2L} \tag{17}$$

where $\boldsymbol{\mathcal{D}}_{x_i}(m)$ is a diagonal matrix whose diagonal elements are given by the DFT of the first column of $\mathbf{C}_{x_i}(m)$, i.e., the overlapped $i$th channel output in the $m$th block

$$\mathbf{x}_i(m)_{2L\times 1} = [x_i(mL-L) \quad x_i(mL-L+1) \quad \cdots \quad x_i(mL+L-1)]^T. \tag{18}$$

Now, we multiply (14) by $\mathbf{F}_{L\times L}$ and use (17) to determine the block error sequence in the frequency domain:

$$\begin{aligned}\underline{\boldsymbol{e}}_{ij}(m) =& \mathbf{F}_{L\times L}\mathbf{e}_{ij}(m)\\ =& \mathbf{F}_{L\times L}\mathbf{W}_{L\times 2L}^{01}\\ &\times\left[\mathbf{C}_{x_i}\mathbf{W}_{2L\times L}^{10}\hat{\mathbf{h}}_j(m) - \mathbf{C}_{x_j}\mathbf{W}_{2L\times L}^{10}\hat{\mathbf{h}}_i(m)\right]\\ =& \boldsymbol{\mathcal{W}}_{L\times 2L}^{01}\\ &\times\left[\boldsymbol{\mathcal{D}}_{x_i}(m)\boldsymbol{\mathcal{W}}_{2L\times L}^{10}\underline{\hat{\boldsymbol{h}}}_j(m) - \boldsymbol{\mathcal{D}}_{x_j}(m)\boldsymbol{\mathcal{W}}_{2L\times L}^{10}\underline{\hat{\boldsymbol{h}}}_i(m)\right]\end{aligned} \tag{19}$$

where

$$\begin{aligned}\boldsymbol{\mathcal{W}}_{L\times 2L}^{01} &= \mathbf{F}_{L\times L}\mathbf{W}_{L\times 2L}^{01}\mathbf{F}_{2L\times 2L}^{-1}\\ \boldsymbol{\mathcal{W}}_{2L\times L}^{10} &= \mathbf{F}_{2L\times 2L}\mathbf{W}_{2L\times L}^{10}\mathbf{F}_{L\times L}^{-1}\end{aligned}$$

and $\underline{\hat{\boldsymbol{h}}}_i(m)$ consists of the $L$-point DFTs of the vector $\hat{\mathbf{h}}_i(m)$ at the $m$th block, i.e., $\underline{\hat{\boldsymbol{h}}}_i(m) = \mathbf{F}_{L\times L}\hat{\mathbf{h}}_i(m)$.

Having derived a frequency-domain block error signal (19), we consequently construct a frequency-domain mean square error criterion analogous to its time-domain counterpart

$$J_f = E\{J_f(m)\} \tag{20}$$

where

$$J_f(m) = \sum_{i=1}^{M-1}\sum_{j=i+1}^{M}\underline{\boldsymbol{e}}_{ij}^{H}(m)\underline{\boldsymbol{e}}_{ij}(m)$$

is the instantaneous square error at the $m$th block.

The LMS algorithm approaches the desired solution by going along the opposite direction of the error's gradient at each iteration step. Taking the partial derivative of $J_f$ with respect to $\underline{\hat{\boldsymbol{h}}}_k^*(m)$, $k = 1, 2, \ldots, M$, we obtain a gradient vector (pretending that $\underline{\hat{\boldsymbol{h}}}_k(m)$ is a constant [17])

$$\frac{\partial J_f}{\partial \underline{\hat{\boldsymbol{h}}}_k^*(m)} = E\left\{\frac{\partial J_f(m)}{\partial \underline{\hat{\boldsymbol{h}}}_k^*(m)}\right\}. \tag{21}$$

In the LMS algorithm, the expectation is estimated with a one-point sample mean, i.e., the instantaneous value, which is given by

$$\begin{aligned}\frac{\partial J_f(m)}{\partial \underline{\hat{\boldsymbol{h}}}_k^*(m)} =& \frac{\partial}{\partial \underline{\hat{\boldsymbol{h}}}_k^*(m)}\left(\sum_{i=1}^{k-1}\underline{\boldsymbol{e}}_{ik}^{H}(m)\underline{\boldsymbol{e}}_{ik}(m)\right)\\ &+\frac{\partial}{\partial \underline{\hat{\boldsymbol{h}}}_k^*(m)}\left(\sum_{j=k+1}^{M}\underline{\boldsymbol{e}}_{kj}^{H}(m)\underline{\boldsymbol{e}}_{kj}(m)\right)\\ =& \sum_{i=1}^{k-1}\left(\boldsymbol{\mathcal{W}}_{L\times 2L}^{01}\boldsymbol{\mathcal{D}}_{x_i}(m)\boldsymbol{\mathcal{W}}_{2L\times L}^{10}\right)^H\underline{\boldsymbol{e}}_{ik}(m)\\ &-\sum_{j=k+1}^{M}\left(\boldsymbol{\mathcal{W}}_{L\times 2L}^{01}\boldsymbol{\mathcal{D}}_{x_j}(m)\boldsymbol{\mathcal{W}}_{2L\times L}^{10}\right)^H\underline{\boldsymbol{e}}_{kj}(m)\\ =& \sum_{i=1}^{M}\left(\boldsymbol{\mathcal{W}}_{L\times 2L}^{01}\boldsymbol{\mathcal{D}}_{x_i}(m)\boldsymbol{\mathcal{W}}_{2L\times L}^{10}\right)^H\underline{\boldsymbol{e}}_{ik}(m)\end{aligned} \tag{22}$$

where the last step follows from the fact $\underline{\boldsymbol{e}}_{kk}(m) = \mathbf{0}$. By using this gradient, we get the frequency-domain LMS algorithm

$$\underline{\hat{\boldsymbol{h}}}_k(m+1) = \underline{\hat{\boldsymbol{h}}}_k(m) - \mu_f\boldsymbol{\mathcal{W}}_{L\times 2L}^{10}\sum_{i=1}^{M}\boldsymbol{\mathcal{D}}_{x_i}^{*}(m)\boldsymbol{\mathcal{W}}_{2L\times L}^{01}\underline{\boldsymbol{e}}_{ik}(m) \tag{23}$$

where $\mu_f$ is a small positive step size, and

$$\begin{aligned}\boldsymbol{\mathcal{W}}_{L\times 2L}^{10} &= \mathbf{F}_{L\times L}\mathbf{W}_{L\times 2L}^{10}\mathbf{F}_{2L\times 2L}^{-1} = \frac{1}{2}\left(\boldsymbol{\mathcal{W}}_{2L\times L}^{10}\right)^H\\ \boldsymbol{\mathcal{W}}_{2L\times L}^{01} &= \mathbf{F}_{2L\times 2L}\mathbf{W}_{2L\times L}^{01}\mathbf{F}_{L\times L}^{-1} = 2\left(\boldsymbol{\mathcal{W}}_{L\times 2L}^{01}\right)^H\\ \mathbf{W}_{L\times 2L}^{10} &= [\mathbf{I}_{L\times L} \quad \mathbf{0}_{L\times L}],\\ \mathbf{W}_{2L\times L}^{01} &= [\mathbf{0}_{L\times L} \quad \mathbf{I}_{L\times L}]^T.\end{aligned}$$

To avoid a trivial estimate with all zero elements, at each step, the time-domain adaptive filter coefficient vector $\hat{\mathbf{h}}(m)$ is constrained to have a unit norm, i.e., $\|\hat{\mathbf{h}}(m)\| = 1$. Equivalently, in the frequency domain, by using (16), we have

$$\|\underline{\hat{\boldsymbol{h}}}(m)\|^2 = \frac{\|\hat{\mathbf{h}}(m)\|^2}{L} = \frac{1}{L} \tag{24}$$

where

$$\underline{\hat{\boldsymbol{h}}}(m) \triangleq \left[\underline{\hat{\boldsymbol{h}}}_1^T(m) \quad \underline{\hat{\boldsymbol{h}}}_2^T(m) \quad \cdots \quad \underline{\hat{\boldsymbol{h}}}_M^T(m)\right]^T.$$

Enforcing the constraint on (23), we finally deduce the multichannel frequency-domain LMS (MCFLMS) algorithm

$$\underline{\hat{\boldsymbol{h}}}_k(m+1) = \frac{\underline{\hat{\boldsymbol{h}}}_k(m) - \mu_f\boldsymbol{\mathcal{W}}_{L\times 2L}^{10}\sum_{i=1}^{M}\boldsymbol{\mathcal{D}}_{x_i}^{*}(m)\boldsymbol{\mathcal{W}}_{2L\times L}^{01}\underline{\boldsymbol{e}}_{ik}(m)}{\sqrt{L}\left\|\underline{\hat{\boldsymbol{h}}}\right\|}, \quad k = 1, 2, \ldots, M. \tag{25}$$

### B. Convergence Analysis

Having developed the multichannel LMS adaptive algorithm in the frequency domain, we need to demonstrate that it would converge in the mean to the desired solution in a stationary environment. To establish this property, we begin by defining

$$\overset{L\times L}{\boldsymbol{\mathcal{S}}_{x_i}(m)} \stackrel{\triangle}{=} \boldsymbol{\mathcal{W}}^{01}_{L\times 2L}\boldsymbol{\mathcal{D}}_{x_i}(m)\boldsymbol{\mathcal{W}}^{10}_{2L\times L},\ i = 1, 2, \ldots, M. \tag{26}$$

By using this matrix, the block error signal given by (19) can be rewritten as

$$\overset{L\times 1}{\underline{\mathbf{e}}_{ij}(m)} = \boldsymbol{\mathcal{S}}_{x_i}(m)\underline{\hat{\mathbf{h}}}_j(m) - \boldsymbol{\mathcal{S}}_{x_j}(m)\underline{\hat{\mathbf{h}}}_i(m) \tag{27}$$

and the instantaneous gradient (22) becomes

$$\frac{\partial J_f(m)}{\partial \underline{\hat{\mathbf{h}}}^*_k(m)} = \sum_{i=1}^{M} \overset{L\times L}{\boldsymbol{\mathcal{S}}^H_{x_i}(m)}\overset{L\times 1}{\underline{\mathbf{e}}_{ik}(m)} = \overset{L\times ML}{\boldsymbol{\mathcal{S}}^H(m)}\overset{ML\times 1}{\underline{\mathbf{e}}_k(m)} \tag{28}$$

where

$$\overset{ML\times L}{\boldsymbol{\mathcal{S}}(m)} \stackrel{\triangle}{=} \left[\boldsymbol{\mathcal{S}}^H_{x_1}(m) \quad \boldsymbol{\mathcal{S}}^H_{x_2}(m) \quad \cdots \quad \boldsymbol{\mathcal{S}}^H_{x_M}(m)\right]^H$$

$$\underset{ML\times 1}{\underline{\mathbf{e}}_k(m)} \stackrel{\triangle}{=} \left[\underline{\mathbf{e}}^T_{1k}(m) \quad \underline{\mathbf{e}}^T_{2k}(m) \quad \cdots \quad \underline{\mathbf{e}}^T_{Mk}(m)\right]^T.$$

From (27), we then decompose the error signal $\underline{\mathbf{e}}_k(m)$ associated with the $k$th channel as

$$\underline{\mathbf{e}}_k(m) = \begin{bmatrix} \boldsymbol{\mathcal{S}}_{x_1}(m)\underline{\hat{\mathbf{h}}}_k(m) - \boldsymbol{\mathcal{S}}_{x_k}(m)\underline{\hat{\mathbf{h}}}_1(m) \\ \boldsymbol{\mathcal{S}}_{x_2}(m)\underline{\hat{\mathbf{h}}}_k(m) - \boldsymbol{\mathcal{S}}_{x_k}(m)\underline{\hat{\mathbf{h}}}_2(m) \\ \vdots \\ \boldsymbol{\mathcal{S}}_{x_M}(m)\underline{\hat{\mathbf{h}}}_k(m) - \boldsymbol{\mathcal{S}}_{x_k}(m)\underline{\hat{\mathbf{h}}}_M(m) \end{bmatrix} = \left[\boldsymbol{\mathcal{U}}_k(m) - \boldsymbol{\mathcal{V}}_k(m)\right]\underline{\hat{\mathbf{h}}}(m) \tag{29}$$

where we have the first equation at the bottom of the page. Continuing, we can write, (30) and (31), shown at the bottom of the page, where

$$\overset{L\times L}{\tilde{\boldsymbol{\mathcal{R}}}_{ij}(m)} \stackrel{\triangle}{=} \boldsymbol{\mathcal{S}}^H_{x_i}(m)\boldsymbol{\mathcal{S}}_{x_j}(m),\ i, j = 1, 2, \ldots, M.$$

Combining the above into (28) and (29) yields (32), shown at the bottom of the page. Substituting this gradient estimate into (23) and concatenating the $M$ impulse response vectors into a longer one produces a remarkably simple expression of the MCFLMS algorithm:

$$\underline{\hat{\mathbf{h}}}(m+1) = \underline{\hat{\mathbf{h}}}(m) - \mu_f\tilde{\boldsymbol{\mathcal{R}}}(m)\underline{\hat{\mathbf{h}}}(m) \tag{33}$$

where we have the equation at the bottom of the next page. With the time-domain unit norm constraint imposed, the MCFLMS algorithm is given by

$$\underline{\hat{\mathbf{h}}}(m+1) = \frac{\underline{\hat{\mathbf{h}}}(m) - \mu_f\tilde{\boldsymbol{\mathcal{R}}}(m)\underline{\hat{\mathbf{h}}}(m)}{\sqrt{L}\left\|\underline{\hat{\mathbf{h}}}(m) - \mu_f\tilde{\boldsymbol{\mathcal{R}}}(m)\underline{\hat{\mathbf{h}}}(m)\right\|}. \tag{34}$$

Subtracting the desired solution $\underline{\mathbf{h}}$ from both sides of (33), we get the evolution of the misalignment in the frequency domain:

$$\Delta\underline{\mathbf{h}}(m+1) = \Delta\underline{\mathbf{h}}(m) - \mu_f\tilde{\boldsymbol{\mathcal{R}}}(m)\underline{\hat{\mathbf{h}}}(m) \tag{35}$$

where

$$\Delta\underline{\mathbf{h}}(m) = \underline{\hat{\mathbf{h}}}(m) - \underline{\mathbf{h}}.$$

Taking the expectation of (35) and invoking the independence assumption [18], i.e., the channel output $\mathbf{x}_i(m)$,

---

$$\boldsymbol{\mathcal{U}}_k(m) = \begin{bmatrix} \mathbf{0}_{L\times L} & \cdots & \mathbf{0}_{L\times L} & \boldsymbol{\mathcal{S}}_{x_1}(m) & \mathbf{0}_{L\times L} & \cdots & \mathbf{0}_{L\times L} \\ \mathbf{0}_{L\times L} & \cdots & \mathbf{0}_{L\times L} & \boldsymbol{\mathcal{S}}_{x_2}(m) & \mathbf{0}_{L\times L} & \cdots & \mathbf{0}_{L\times L} \\ \vdots & \cdots & \vdots & \vdots & \vdots & \cdots & \vdots \\ \underbrace{\mathbf{0}_{L\times L}}_{} & \underbrace{\cdots}_{k-1\ blocks} & \underbrace{\mathbf{0}_{L\times L}}_{} & \boldsymbol{\mathcal{S}}_{x_M}(m) & \underbrace{\mathbf{0}_{L\times L}}_{} & \underbrace{\cdots}_{M-k\ blocks} & \underbrace{\mathbf{0}_{L\times L}}_{} \end{bmatrix}_{ML\times ML}$$

$$= \left[\mathbf{0}_{ML\times(k-1)L} \quad \boldsymbol{\mathcal{S}}(m) \quad \mathbf{0}_{ML\times(M-k)L}\right]_{ML\times ML}$$

$$\boldsymbol{\mathcal{V}}_k(m) = \begin{bmatrix} \boldsymbol{\mathcal{S}}_{x_k}(m) & \mathbf{0}_{L\times L} & \cdots & \mathbf{0}_{L\times L} \\ \mathbf{0}_{L\times L} & \boldsymbol{\mathcal{S}}_{x_k}(m) & \cdots & \mathbf{0}_{L\times L} \\ \vdots & \vdots & \ddots & \vdots \\ \mathbf{0}_{L\times L} & \mathbf{0}_{L\times L} & \cdots & \boldsymbol{\mathcal{S}}_{x_k}(m) \end{bmatrix}_{ML\times ML}.$$

---

$$\begin{aligned} \boldsymbol{\mathcal{S}}^H(m)\boldsymbol{\mathcal{U}}_k(m) &= \overset{L\times ML}{\boldsymbol{\mathcal{S}}^H(m)}\left[\mathbf{0}_{L\times(k-1)L} \quad \overset{ML\times L}{\boldsymbol{\mathcal{S}}(m)} \quad \mathbf{0}_{L\times(M-k)L}\right] \\ &= \left[\mathbf{0}_{L\times(k-1)L} \quad \sum_{i=1}^{M}\tilde{\boldsymbol{\mathcal{R}}}_{ii}(m) \quad \mathbf{0}_{L\times(M-k)L}\right]_{L\times ML} \end{aligned} \tag{30}$$

$$\boldsymbol{\mathcal{S}}^H(m)\boldsymbol{\mathcal{V}}_k(m) = \left[\tilde{\boldsymbol{\mathcal{R}}}_{1k}(m) \quad \tilde{\boldsymbol{\mathcal{R}}}_{2k}(m) \quad \cdots \quad \tilde{\boldsymbol{\mathcal{R}}}_{Mk}(m)\right]. \quad L\times ML \tag{31}$$

---

$$\begin{aligned} \frac{\partial J_f(m)}{\partial \underline{\hat{\mathbf{h}}}^*_k(m)} &= \boldsymbol{\mathcal{S}}^H(m)\left[\boldsymbol{\mathcal{U}}_k(m) - \boldsymbol{\mathcal{V}}_k(m)\right]\underline{\hat{\mathbf{h}}}(m) \\ &= \left[-\tilde{\boldsymbol{\mathcal{R}}}_{1k}(m) - \tilde{\boldsymbol{\mathcal{R}}}_{2k}(m) \quad \cdots \quad \sum_{i\neq k}\tilde{\boldsymbol{\mathcal{R}}}_{ii}(m) \quad \cdots \quad -\tilde{\boldsymbol{\mathcal{R}}}_{Mk}(m)\right]\underline{\hat{\mathbf{h}}}(m). \end{aligned} \tag{32}$$

$i = 1, 2, \ldots, M$, and the filter coefficients $\underline{\hat{\boldsymbol{h}}}(m)$ are independent, we have

$$E\left\{\Delta\underline{\boldsymbol{h}}(m+1)\right\} = E\left\{\Delta\underline{\boldsymbol{h}}(m)\right\} - \mu_f \boldsymbol{\mathcal{R}} \cdot E\left\{\underbrace{\underline{\hat{\boldsymbol{h}}}(m)}_{\Delta h(m)}\right\} \quad (36)$$

$= E[\Delta h(m)] - \mu R E[\hat{h}(m) - h]$

where

$$\boldsymbol{\mathcal{R}} = E\left\{\tilde{\boldsymbol{\mathcal{R}}}(m)\right\}.$$

Recall that the gradient of the mean square error is zero for the desired solution, i.e.,

$$\frac{\partial J_f}{\partial \underline{\boldsymbol{h}}} = \boldsymbol{\mathcal{R}}\underline{\boldsymbol{h}} = \mathbf{0}$$

with which (36) becomes

$$E\left\{\Delta\underline{\boldsymbol{h}}(m+1)\right\} = \left(\mathbf{I}_{ML\times ML} - \mu_f \boldsymbol{\mathcal{R}}\right) E\left\{\Delta\underline{\boldsymbol{h}}(m)\right\}. \quad (37)$$

Therefore, if the step-size satisfies

$$0 < \mu_f < \frac{2}{\lambda_{\max}} \quad (38)$$

where $\lambda_{\max}$ is the largest eigenvalue of the matrix $\boldsymbol{\mathcal{R}}$, then the misalignment mean $E\{\Delta\underline{\boldsymbol{h}}(m)\}$ converges to zero, and the estimated filter coefficients converge in the mean to the desired solutions.

## IV. Normalized Multichannel Frequency-Domain LMS Algorithms

Compared with a multichannel time-domain block LMS algorithm, the MCFLMS is computationally more efficient since it uses the FFT to calculate block convolution and block correlation in the frequency domain. For each processed frame $(M^2 + 2M)$, FFTs of $2L$ points are sufficient to implement exact linear convolutions between the channel outputs and the adaptive filter coefficients and to implement exact correlations between the outputs and the error signals. Although the algorithm converges to the optimal solution, its convergence is slow because of nonuniform convergence rates of the filter coefficients and cross-coupling between them. In this section, Newton's method will first be used, and then, necessary simplifications will be taken advantage of to develop a normalized multichannel frequency-domain LMS (NMCFLMS) algorithm for which the eigenvalue disparity is reduced, and the convergence is accelerated.

To utilize Newton's method, we will evaluate the Hessian matrix of $J_f$ with respect to the filter coefficients, which can be computed as follows by taking the row gradient of (28)

$$\begin{aligned}\boldsymbol{\mathcal{T}}_k(m) =& \frac{\partial}{\partial \underline{\hat{\boldsymbol{h}}}_k^T(m)}\left[\frac{\partial J_f}{\partial \underline{\hat{\boldsymbol{h}}}_k^*(m)}\right] = \frac{\partial}{\partial \underline{\hat{\boldsymbol{h}}}_k^T(m)}\left[\boldsymbol{\mathcal{S}}^H(m)\underline{\boldsymbol{e}}_k(m)\right]\\ =& \boldsymbol{\mathcal{S}}^H(m)\frac{\partial \underline{\boldsymbol{e}}_k(m)}{\partial \underline{\hat{\boldsymbol{h}}}_k(m)}\\ =& \sum_{i=1, i\neq k}^{M} \boldsymbol{\mathcal{S}}_{x_i}^H(m)\boldsymbol{\mathcal{S}}_{x_i}(m)\end{aligned} \quad (39)$$

with which the filter coefficient update (23) is modified to

$$\begin{aligned}\underline{\hat{\boldsymbol{h}}}_k(m+1) =& \underline{\hat{\boldsymbol{h}}}_k(m) - \rho\boldsymbol{\mathcal{T}}_k^{-1}(m)\boldsymbol{\mathcal{S}}^H(m)\underline{\boldsymbol{e}}_k(m)\\ =& \underline{\hat{\boldsymbol{h}}}_k(m) - \rho\boldsymbol{\mathcal{T}}_k^{-1}(m)\boldsymbol{\mathcal{W}}_{L\times 2L}^{10}\\ &\times \sum_{i=1}^{M}\boldsymbol{\mathcal{D}}_{x_i}^*(m)\boldsymbol{\mathcal{W}}_{2L\times L}^{01}\underline{\boldsymbol{e}}_{ik}(m)\\ & k = 1, 2, \ldots, M\end{aligned} \quad (40)$$

where $\rho$ is a new step size. Of course, the constraint (24) needs to be enforced, but for ease of presentation, such an operation will not be explicitly specified starting from this section. If we multiply (40) by $\boldsymbol{\mathcal{W}}_{2L\times L}^{10}$, we obtain Newton's algorithm:

$$\begin{aligned}\underline{\hat{\boldsymbol{h}}}_k^{10}(m+1) =& \underline{\hat{\boldsymbol{h}}}_k^{10}(m) - \rho\boldsymbol{\mathcal{W}}_{2L\times L}^{10}\boldsymbol{\mathcal{T}}_k^{-1}(m)\boldsymbol{\mathcal{W}}_{L\times 2L}^{10}\\ &\times\sum_{i=1}^{M}\boldsymbol{\mathcal{D}}_{x_i}^*(m)\underline{\boldsymbol{e}}_{ik}^{01}(m),\ k = 1, 2, \ldots, M\end{aligned} \quad (41)$$

where

$$\begin{aligned}\underline{\hat{\boldsymbol{h}}}_k^{10}(m) =& \boldsymbol{\mathcal{W}}_{2L\times L}^{10}\underline{\hat{\boldsymbol{h}}}_k(m) = \mathbf{F}_{2L\times 2L}\begin{bmatrix}\hat{\mathbf{h}}_k(m)\\ \mathbf{0}\end{bmatrix}\\ \underline{\boldsymbol{e}}_{ik}^{01}(m) =& \boldsymbol{\mathcal{W}}_{2L\times L}^{01}\underline{\boldsymbol{e}}_{ik}(m) = \mathbf{F}_{2L\times 2L}\begin{bmatrix}\mathbf{0}\\ \mathbf{F}_{L\times L}^{-1}\underline{\boldsymbol{e}}_{ik}(m)\end{bmatrix}.\end{aligned}$$

Such a frequency-domain Newton's algorithm is able to converge quickly. Unfortunately, however, the matrix $\boldsymbol{\mathcal{T}}_k(m)$ is not diagonal, and finding its inverse involves too much complexity, particularly when $L$ is large.

Thus far, the discussion has indicated that we must face a tradeoff between complexity and convergence rate when designing a multichannel frequency-domain adaptive filter. It would, of course, be advantageous to have an algorithm that combines the low complexity of the MCFLMS approach and the fast convergence of the Newton's method. The NMCFLMS can be seen as an attempt to achieve this compromise.

---

$$\tilde{\boldsymbol{\mathcal{R}}}(m) = \begin{bmatrix}\sum_{i\neq 1}\tilde{\boldsymbol{\mathcal{R}}}_{ii}(m) & -\tilde{\boldsymbol{\mathcal{R}}}_{21}(m) & \cdots & -\tilde{\boldsymbol{\mathcal{R}}}_{M1}(m)\\ -\tilde{\boldsymbol{\mathcal{R}}}_{12}(m) & \sum_{i\neq 2}\tilde{\boldsymbol{\mathcal{R}}}_{ii}(m) & \cdots & -\tilde{\boldsymbol{\mathcal{R}}}_{M2}(m)\\ \vdots & \vdots & \ddots & \vdots\\ -\tilde{\boldsymbol{\mathcal{R}}}_{1M}(m) & -\tilde{\boldsymbol{\mathcal{R}}}_{2M}(m) & \cdots & \sum_{i\neq M}\tilde{\boldsymbol{\mathcal{R}}}_{ii}(m)\end{bmatrix}_{ML\times ML}.$$

Let us expand the product in (39) using the definition (26) to find

$$\boldsymbol{\mathcal{S}}_{x_i}^H(m)\boldsymbol{\mathcal{S}}_{x_i}(m) = \boldsymbol{\mathcal{W}}_{L\times 2L}^{10}\boldsymbol{\mathcal{D}}_{x_i}^*(m)\boldsymbol{\mathcal{W}}_{2L\times 2L}^{01}\boldsymbol{\mathcal{D}}_{x_i}(m)\boldsymbol{\mathcal{W}}_{2L\times L}^{10} \tag{42}$$

where

$$\begin{aligned}\boldsymbol{\mathcal{W}}_{2L\times 2L}^{01} &\triangleq \boldsymbol{\mathcal{W}}_{2L\times L}^{01}\boldsymbol{\mathcal{W}}_{L\times 2L}^{01}\\ &= \mathbf{F}_{2L\times 2L}\begin{bmatrix}\mathbf{0}_{L\times L} & \mathbf{0}_{L\times L}\\ \mathbf{0}_{L\times L} & \mathbf{I}_{L\times L}\end{bmatrix}\mathbf{F}_{2L\times 2L}^{-1}\end{aligned}$$

whose elements on its main diagonal dominate, as shown in [19]. When $L$ is large, $2\boldsymbol{\mathcal{W}}_{2L\times 2L}^{01}$ can be well approximated by the identity matrix

$$2\boldsymbol{\mathcal{W}}_{2L\times 2L}^{01} \approx \mathbf{I}_{2L\times 2L}. \tag{43}$$

Therefore, (42) becomes

$$\boldsymbol{\mathcal{S}}_{x_i}^H(m)\boldsymbol{\mathcal{S}}_{x_i}(m) \approx \frac{1}{2}\boldsymbol{\mathcal{W}}_{L\times 2L}^{10}\boldsymbol{\mathcal{D}}_{x_i}^*(m)\boldsymbol{\mathcal{D}}_{x_i}(m)\boldsymbol{\mathcal{W}}_{2L\times L}^{10} \tag{44}$$

and (39) turns into

$$\begin{aligned}\boldsymbol{\mathcal{T}}_k(m) &\approx \frac{1}{2}\boldsymbol{\mathcal{W}}_{L\times 2L}^{10}\left[\sum_{i=1,i\neq k}^{M}\boldsymbol{\mathcal{P}}_{x_i}(m)\right]\boldsymbol{\mathcal{W}}_{2L\times L}^{10}\\ &= \frac{1}{2}\boldsymbol{\mathcal{W}}_{L\times 2L}^{10}\boldsymbol{\mathcal{P}}_k(m)\boldsymbol{\mathcal{W}}_{2L\times L}^{10}\end{aligned} \tag{45}$$

where

$$\begin{aligned}\boldsymbol{\mathcal{P}}_{x_i}(m) &= \boldsymbol{\mathcal{D}}_{x_i}^*(m)\boldsymbol{\mathcal{D}}_{x_i}(m)\\ \boldsymbol{\mathcal{P}}_k(m) &= \sum_{i=1,i\neq k}^{M}\boldsymbol{\mathcal{P}}_{x_i}(m),\ k=1,2,\ldots,M\end{aligned}$$

which are diagonal matrices. There is a useful relation between the inverses of the $\boldsymbol{\mathcal{T}}_k(m)$ and $\boldsymbol{\mathcal{P}}_k(m)$ matrices given by [19]

$$\boldsymbol{\mathcal{W}}_{2L\times L}^{10}\boldsymbol{\mathcal{T}}_k^{-1}(m)\boldsymbol{\mathcal{W}}_{L\times 2L}^{10} = 2\boldsymbol{\mathcal{W}}_{2L\times 2L}^{10}\boldsymbol{\mathcal{P}}_k^{-1}(m) \tag{46}$$

where

$$\boldsymbol{\mathcal{W}}_{2L\times 2L}^{10} = \boldsymbol{\mathcal{W}}_{2L\times L}^{10}\boldsymbol{\mathcal{W}}_{L\times 2L}^{10}.$$

This relation can be justified by post-multiplying both sides of the expression by $\boldsymbol{\mathcal{P}}_k(m)\boldsymbol{\mathcal{W}}_{2L\times L}^{10}$, using (45), and recognizing that

$$\boldsymbol{\mathcal{W}}_{2L\times 2L}^{10}\boldsymbol{\mathcal{W}}_{2L\times L}^{10} = \boldsymbol{\mathcal{W}}_{2L\times L}^{10}.$$

Substituting (46) into (41) gives the *constrained* NMCFLMS algorithm

$$\begin{aligned}\underline{\hat{\boldsymbol{h}}}_k^{10}(m+1) &= \underline{\hat{\boldsymbol{h}}}_k^{10}(m) - 2\rho\boldsymbol{\mathcal{W}}_{2L\times 2L}^{10}\boldsymbol{\mathcal{P}}_k^{-1}(m)\\ &\quad\times\sum_{i=1}^{M}\boldsymbol{\mathcal{D}}_{x_i}^*(m)\underline{\boldsymbol{e}}_{ik}^{01}(m),\ k=1,2,\ldots,M.\end{aligned} \tag{47}$$

If the matrix $2\boldsymbol{\mathcal{W}}_{2L\times 2L}^{10}$ is approximated by the identity matrix similar to (43), we finally deduce the *unconstrained* NMCFLMS algorithm:

$$\begin{aligned}\underline{\hat{\boldsymbol{h}}}_k^{10}(m+1) &= \underline{\hat{\boldsymbol{h}}}_k^{10}(m) - \rho\boldsymbol{\mathcal{P}}_k^{-1}(m)\\ &\quad\times\sum_{i=1}^{M}\boldsymbol{\mathcal{D}}_{x_i}^*(m)\underline{\boldsymbol{e}}_{ik}^{01}(m),\ k=1,2,\ldots,M.\end{aligned} \tag{48}$$

An interesting interpretation follows if we compare the unconstrained NMCFLSM approach (48) with the MCFLMS algorithm (23). In the MCFLMS algorithm, the correction that is applied to $\underline{\hat{\boldsymbol{h}}}_k(m)$ is approximately proportional to the power spectrum $\boldsymbol{\mathcal{P}}_k(m)$ of the multiple channel outputs; this can be seen from (23) and the definition of $\boldsymbol{\mathcal{P}}_k(m)$, making the approximation $2\boldsymbol{\mathcal{W}}_{2L\times 2L}^{01} \approx \mathbf{I}_{2L\times 2L}$. When the channel outputs are large, the gradient noise amplification may be experienced. With the normalization of the MCFLMS correction by $\boldsymbol{\mathcal{P}}_k(m)$ in the NMCFLMS algorithm, this noise amplification problem is diminished, and the variability of the convergence rates due to the change of signal level is eliminated. In order to estimate a more stable power spectrum, a recursive scheme is employed in practice:

$$\begin{aligned}\boldsymbol{\mathcal{P}}_k(m) &= \lambda\boldsymbol{\mathcal{P}}_k(m-1) + (1-\lambda)\\ &\quad\times\sum_{i=1,i\neq k}^{M}\boldsymbol{\mathcal{D}}_{x_i}^*(m)\boldsymbol{\mathcal{D}}_{x_i}(m),\ k=1,2,\ldots,M\end{aligned} \tag{49}$$

where $\lambda$ is a forgetting factor that may appropriately be set as $\lambda = [1-1/(3L)]^L$ for this NMCFLMS algorithm. Although the NMCFLMS algorithm bypasses the problem of noise amplification, we are now faced with a similar problem that occurs when the channel outputs becomes too small. An alternative, therefore, is to insert a small positive number $\delta$ into the normalization, which leads to the following modification to the unconstrained NMCFLMS algorithm:

$$\begin{aligned}\underline{\hat{\boldsymbol{h}}}_k^{10}(m+1) &= \underline{\hat{\boldsymbol{h}}}_k^{10}(m) - \rho\left[\boldsymbol{\mathcal{P}}_k(m) + \delta\mathbf{I}_{2L\times 2L}\right]^{-1}\\ &\quad\times\sum_{i=1}^{M}\boldsymbol{\mathcal{D}}_{x_i}^*(m)\underline{\boldsymbol{e}}_{ik}^{01}(m),\ k=1,2,\ldots,M.\end{aligned} \tag{50}$$

From a computational point of view, the unconstrained NMCFLMS algorithm can be easily implemented, even for a real-time application since the normalization matrix $\boldsymbol{\mathcal{P}}_k(m) + \delta\mathbf{I}_{2L\times 2L}$ is diagonal, and it is straightforward to find its inverse.

## V. Simulations

We have motivated and proposed a class of frequency-domain adaptive approaches to the blind multichannel identification problem, aiming to achieve a compromise of fast convergence, adaptivity, and low computational complexity. Monte Carlo simulations are now presented for evaluating the two novel methods, namely, the MCFLMS and the NMCFLMS algorithms, which have been developed in the previous sections. For comparison, their time-domain counterparts, i.e., the MCLMS and the MCN algorithms, and a batch cross-relation (CR) method are studied.

### A. Performance Measures and Experiment Setup

The normalized root mean square projection misalignment (NRMSPM) in decibels is used as a performance measure of estimation accuracy in this paper and is given by

$$\text{NRMSPM} \triangleq 20\log_{10}\left[\frac{1}{\|\mathbf{h}\|}\sqrt{\frac{1}{N}\sum_{i=1}^{N}\left\|\boldsymbol{\epsilon}^{(i)}\right\|^2}\right] \tag{51}$$

where $N$ is the number of Monte Carlo runs, $(\cdot)^{(i)}$ denotes a value obtained for the $i$th run, and

$$\boldsymbol{\epsilon} = \mathbf{h} - \frac{\mathbf{h}^T\hat{\mathbf{h}}}{\hat{\mathbf{h}}^T\hat{\mathbf{h}}}\hat{\mathbf{h}}$$

is the *projection misalignment* vector. By projecting $\mathbf{h}$ onto $\hat{\mathbf{h}}$ and defining a projection error, we take into account only the intrinsic misalignment of the channel estimate, disregarding an arbitrary gain factor [20].

For a common floating-point implementation of an algorithm, the floating-point operations (flops) dominate the calculation, and the number of flops is a consistent measure of the algorithm's computational complexity, independent of the machine on which it runs. In this paper, the flops per set of multichannel outputs are counted. The absolute number of flops for the studied adaptive algorithms are not particularly meaningful, but their relative values illustrate the great efficiency of the frequency-domain approaches.

In the simulations, two source signals are considered. One is an uncorrelated binary phase-shift-keying (BPSK) sequence, and the other is clean speech. The additive noise is i.i.d. zero-mean Gaussian, and the specified SNR is defined as

$$\text{SNR} \triangleq 10\log_{10}\frac{\sigma_s^2\|\mathbf{h}\|^2}{M\sigma_b^2} \tag{52}$$

where $\sigma_s^2$ and $\sigma_b^2$ are the signal and background noise powers, respectively.

### B. Initialization

How to initialize an adaptive algorithm is always important to its convergence. In general, the better the estimated parameters are guessed, the faster the adaptive algorithm converges. However, *a priori* knowledge of the estimated system is difficult, if not impossible, to obtain for a blind channel identification algorithm in practice. In order to fairly evaluate the proposed methods, a simple initialization was employed for all experiments conducted in this paper. In the time domain, the channel impulse response of the $k$th channel is set as

$$\hat{\mathbf{h}}_k(0) = [1 \quad 0 \quad \cdots \quad 0]^T,\ k = 1, 2, \ldots, M. \tag{53}$$

Then, the overall channel impulse response vector $\mathbf{h}(0)$ is normalized by $\sqrt{M}$ to satisfy the unit-norm constraint as

$$\hat{\mathbf{h}}(0) = \frac{\hat{\mathbf{h}}(0)}{\sqrt{M}}. \tag{54}$$

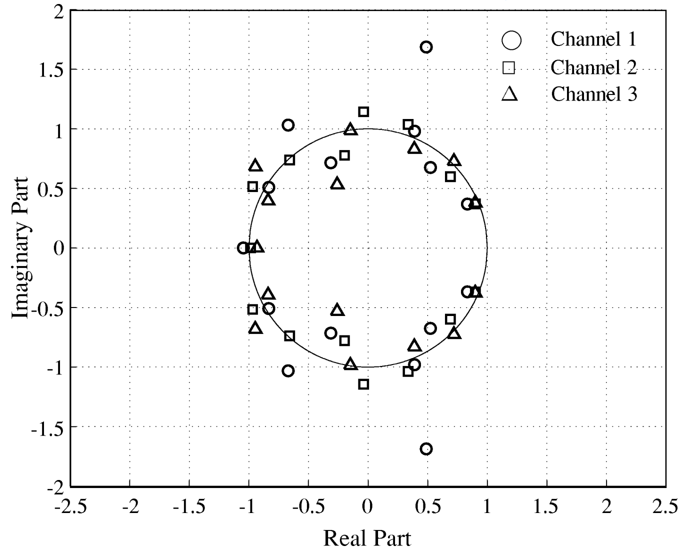


Fig. 3. Illustration of the positions of the channel zeros in the $z$-plane for a random three-channel system.

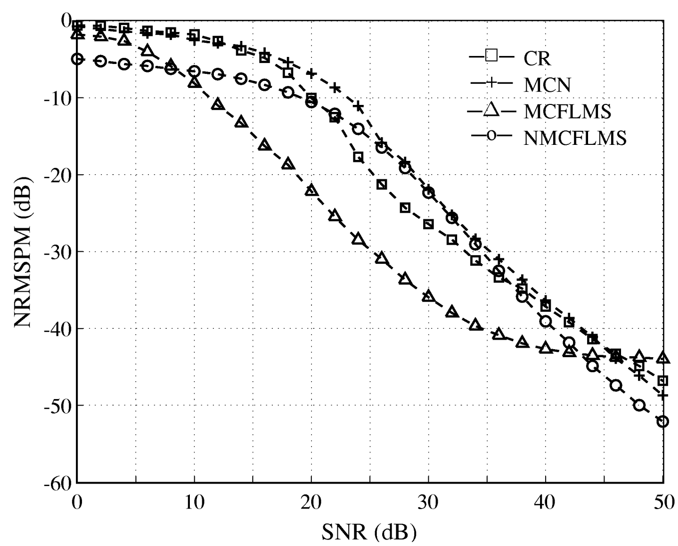


Fig. 4. Comparison of converged NRMSPM versus SNR among the CR, MCN, MCFLMS, and NMCFLMS algorithms for the random three-channel system ($L = 16$) of Fig. 3, excited by a random BPSK sequence.

Equivalently, in the frequency domain, the filter coefficients are all set as $1/\sqrt{M}$. Since the initial channel estimates are identical, a nonzero error signal can be guaranted, and hence, the channel filter coefficients will be properly adapted.

### C. Random Multichannel System

In this simulation, a three-channel system of order $L = 16$ was studied. The coefficients of its impulse responses were randomly determined, and the zeros of each channel are shown in Fig. 3.

First, we consider an uncorrelated BPSK sequence as the source signal to excite the multichannel system. For the CR method, 120 samples of observations from each channel were utilized. For the MCN and MCFLMS algorithms, the step size $\rho = 0.95$ and $\mu_f = 4 \times 10^{-4}$ were fixed, respectively. For the NMCFLMS algorithm, the step size $\rho = 0.8$ was used, and the

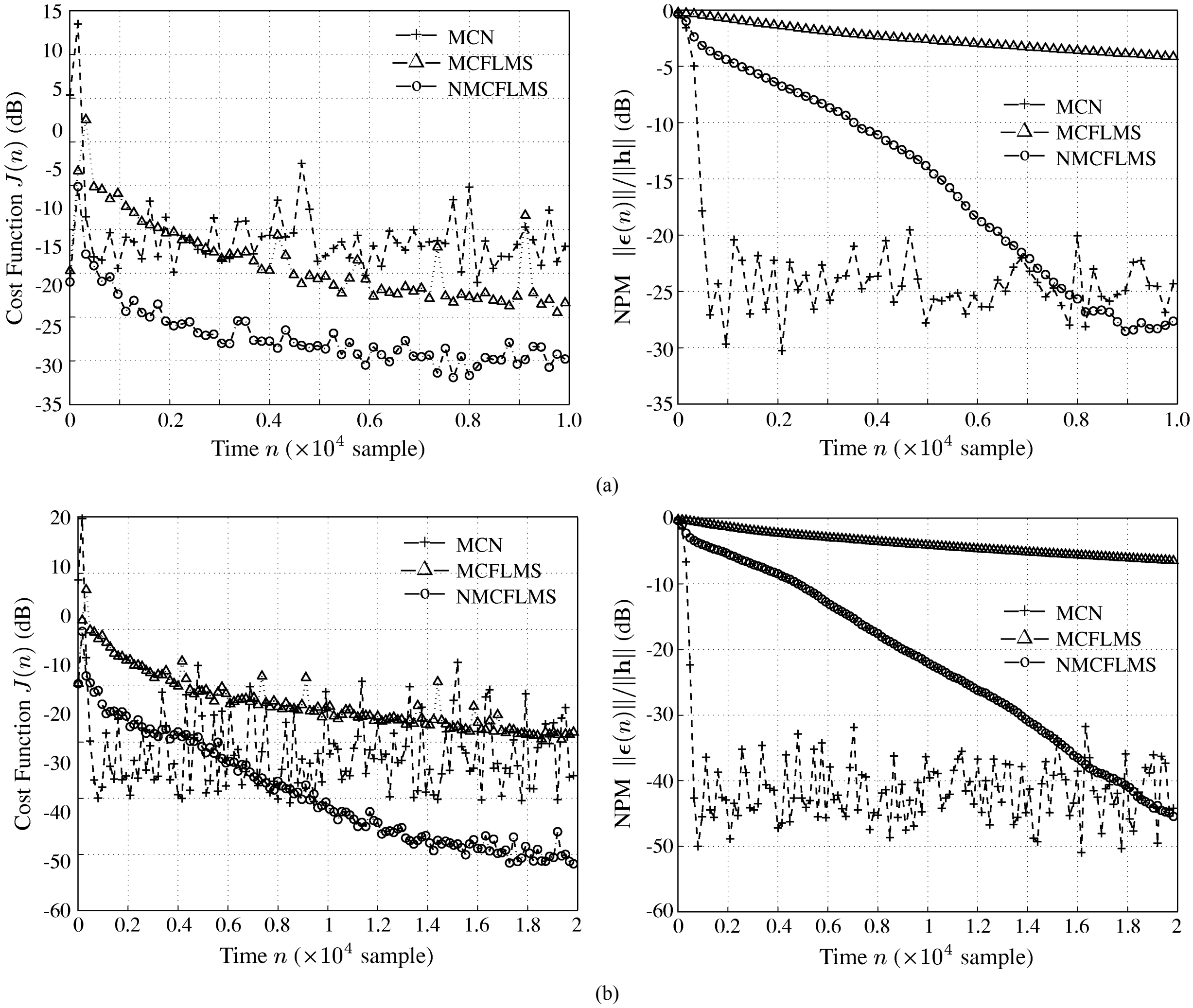


Fig. 5. Comparison of convergence among the MCN, MCFLMS, and NMCFLMS algorithms for the random three-channel system ($L = 16$) of Fig. 3 excited by a random BPSK sequence. Trajectories of the cost function $J(n)$ (left column) and the normalized projection misalignment (NPM) $\|\epsilon(n)\|/\|\mathbf{h}\|$ (right column) versus time $n$ are shown for one typical run of the three algorithms. (a) $SNR = 30$ dB. (b) $SNR = 50$ dB.

regularization factor $\delta$ was initially set as one fifth of the total power over all channels at the first block. For each specified SNR value, the NRMSPM was calculated by averaging the results, after convergence, of $N = 200$ Monte Carlo runs. A comparison of the NRMSPMs among the CR, MCN, MCFLMS, and NMCFLMS algorithms is presented in Fig. 4. In this case, the NRMSPMs of all studied algorithms decrease steadily as the SNR increases. The trajectories of the cost function $J(n)$ and the normalized projection error $\|\epsilon(n)\|/\mathbf{h}$ for one typical run of the adaptive MCN, MCFLMS, and NMCFLMS algorithms are presented for 30- and 50–dB SNRs in Fig. 5(a) and (b), respectively, to compare their convergence. Among the three adaptive methods, the MCN algorithm converges fastest, but on the other hand, the variance of its cost function is also the largest after convergence. Although both the MCFLMS and NMCFLMS algorithms converge steadily to the desired channel impulse responses, apparently, the NMCFLMS algorithm performs better, achieving a good compromise between fast convergence speed and low estimate variance.

Second, a male speech signal sampled at 8 kHz was used as the source to excite the same random three-channel system. The utterance consists of the following sentences:

> "And my problem right now is on the Jones. Jones currently has five RA85 disk drives and four Eagle disk drives. …"

Fig. 6 shows the first 50 000 samples of the signal waveform. As clearly seen from this snapshot, the speech source signal is inherently nonstationary, which makes the blind channel identification problem more difficult for the adaptive algorithms. Because of its slow convergence, the MCFLMS algorithm completely failed to yield a good channel estimate at all SNRs up to 50 dB and with different tested step sizes. For the CR, MCN, and NMCFLMS algorithms, the channel impulse responses are accurately determined when the SNR is high. A comparison of the NRMSPMs among these methods is given in Fig. 7. Again, $N = 200$ Monte Carlo trials were performed at each SNR. For the CR method, 120 samples of observations from each channel were employed. For the MCN and NMCFLMS algorithms, smaller step sizes $\rho = 0.5$ and $\rho = 0.3$ were used, respectively. The regularization factor $\delta$ was set in the same way as that in the first experiment. The nonstationary speech source signal deteriorates the performance of all investigated algorithms. In comparison, the NMCFLMS algorithm is more reliable and stays head and shoulders above the rest, particularly

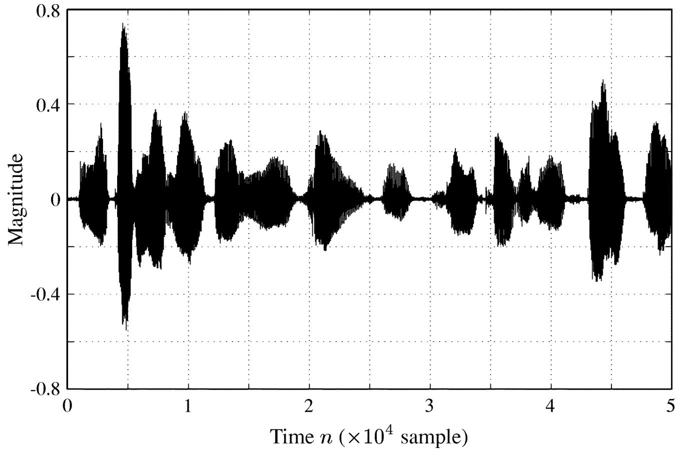


Fig. 6. Male speech signal sampled at 8 kHz.

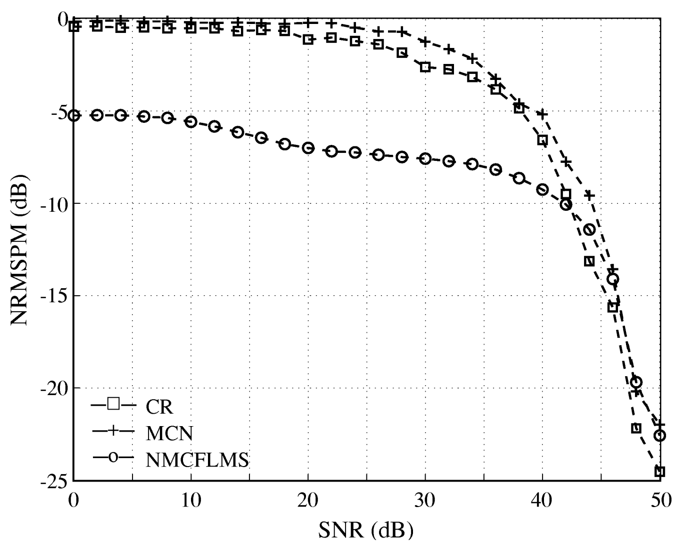


Fig. 7. Comparison of NRMSE versus SNR among the CR, MCN, and NMCFLMS algorithms for the three-channel system with random channel impulse responses ($L = 16$) and excited by the male speech signal of Fig. 6.

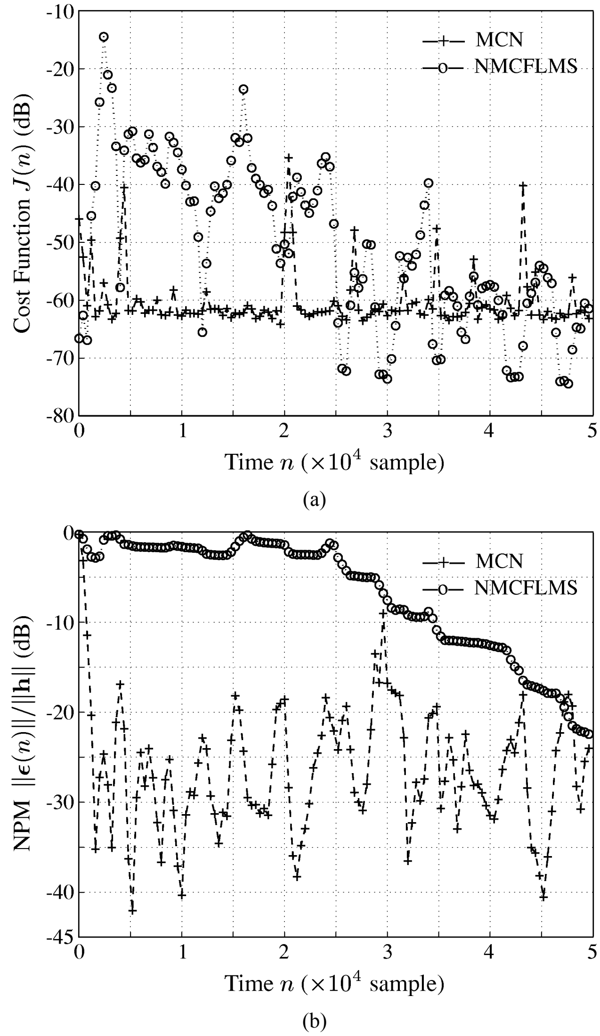


Fig. 8. Comparison of convergence between the MCN and NMCFLMS algorithms for the random three-channel system ($L = 16$) of Fig. 3 excited by the male speech signal of Fig. 6 at 50 dB SNR. (a) Trajectories of the cost function $J(n)$ and (b) the normalized projection misalignment (NPM) $\|\epsilon(n)\|/\|\mathbf{h}\|$ versus time $n$ are shown for one typical run of the two algorithms.

when the SNR is low. A comparison of convergence between the MCN and NMCFLMS algorithms is given in Fig. 8. Fig. 8(a) and (b) presents, respectively, the trajectories of the cost function $J(n)$ and the normalized projection misalignment (NPM) $\|\epsilon(n)\|/\|\mathbf{h}\|$ versus time $n$ for a typical run of these two algorithms. In this case, the instantaneous values of the cost function for the NMCFLMS algorithm fluctuate with each burst of speech energy, whereas its mean converges, but the projection misalignment decreases steadily.

Finally, in Fig. 9, there is a comparison of computational complexity among the MCLMS, MCN, MCFLMS, and NMCFLMS algorithms for random three-channel systems of different order. As the order of the adaptive filter increases, the flops per set of multichannel outputs for the MCN algorithm grow explosively since at each update, a nondiagonal matrix needs to be inverted. Obviously, the frequency-domain adaptive approaches are much more efficient than their time-domain counterparts, especially when $L$ is large. Remarkably, the flops of the proposed frequency-domain algorithms increase just slightly with $L$. The difference in computational complexity between the MCFLMS and NMCFLMS is indistinguishable.

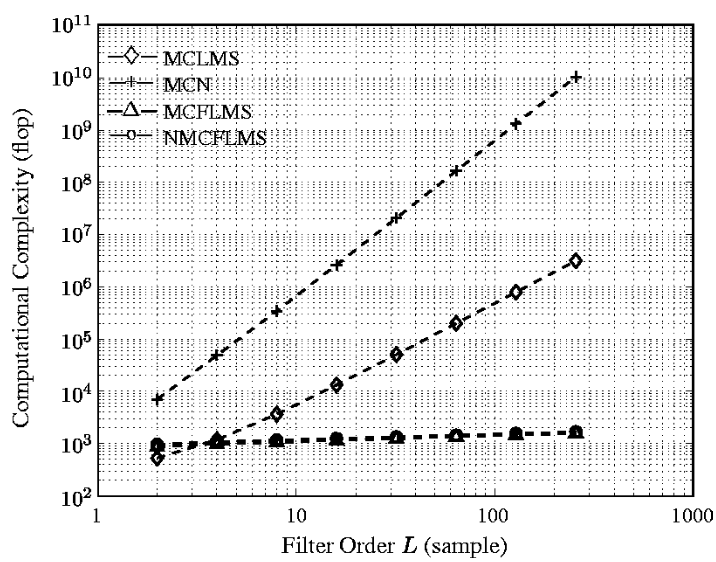


Fig. 9. Comparison of computational complexity per set of multichannel outputs among the MCLMS, MCN, MCFLMS, and NMCFLMS algorithms for three-channel systems with random channel impulse responses of different order, excited by a random BPSK sequence.

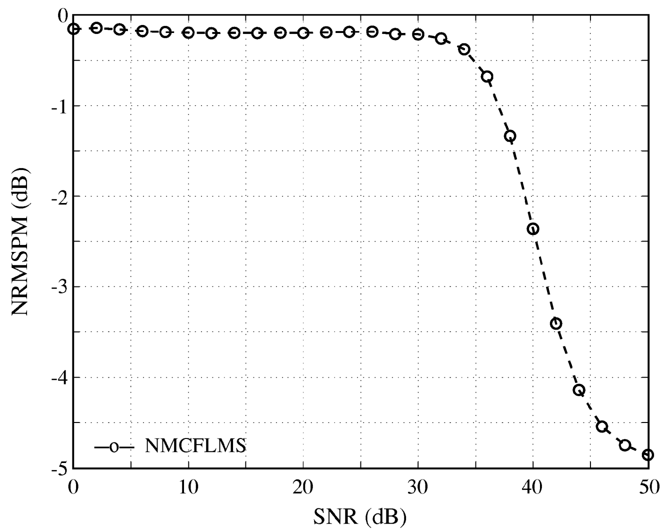


Fig. 10. Performance of the NMCFLMS algorithm measured by the NRMSE versus SNR for the simulated reverberant acoustic three-channel system, excited by the male speech signal of Fig. 6.

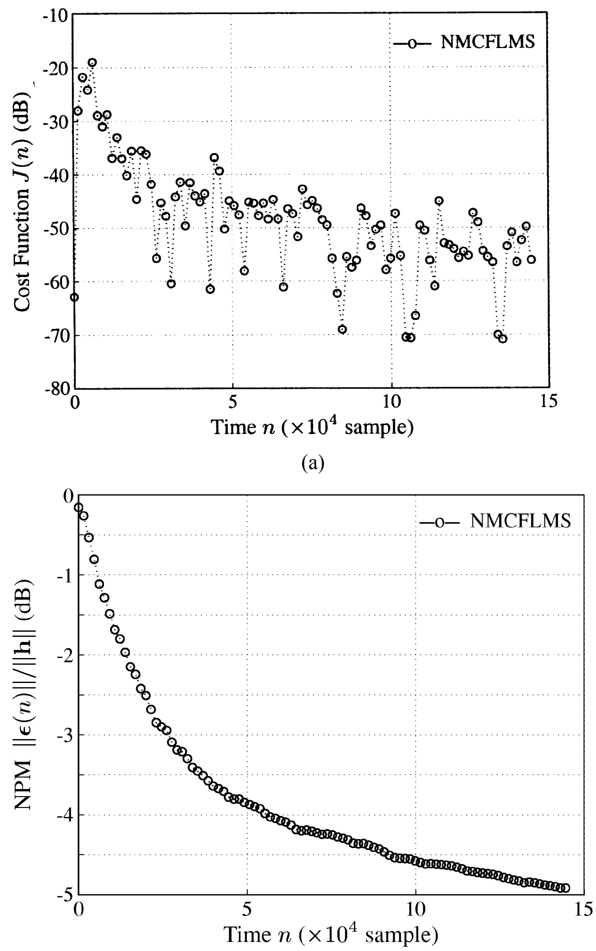


Fig. 11. (a) Trajectories of the cost function $J(n)$ and (b) the normalized projection misalignment (NPM) $||\epsilon(n)||/||\mathbf{h}||$ versus time $n$ for one typical run of the NMCFLMS algorithm for the simulated reverberant acoustic three-channel system, excited by the male speech signal of Fig. 6 at 50 dB SNR.

### D. Real Reverberant Acoustic Multichannel System

In an attempt to evaluate the performance of the proposed blind channel identification algorithms in a real reverberant acoustic environment, we artifically generate impulse responses for a small room using the image method [15]. The small room imitates the enclosure of a car and is of size 70 $\times$ 80 $\times$ 30 in ($x \times y \times z$). A single source is located at (50, 60, 15), and three employed sensors (microphones) are set at (10, 10, 25), (35, 10, 25), and (60, 10, 25), respectively. The wall reflection coefficients are 0.8, and the floor and ceiling reflection coefficients are 0.5. Since a group delay in all channels has no influence on the blind channel identification problem, we align the impulse responses of the three channels such that the first tap of at least one channel is not zero, which makes the comparison of the real and estimated channel impulse responses more reasonable. The sampling rate is 8 kHz. For each channel, the filter order is set as $L = 256$ such that most of the reverberation is taken into account, as is clearly shown in the plots. The male speech signal of Fig. 6 was again used as source.

Blindly estimating such an acoustic multichannel system is a big challenge for all existing methods that focus primarily on short communication channels. In this simulation, up to 3000 samples were employed to test the CR algorithm. We noticed that it was very burdensome to perform singular value decomposition (SVD) in the CR method using an Intel Pentium III 1 GHz PC equipped with 256-MB memory when 3000 samples were used. Moreover, a good estimate cannot be found even at 50 dB SNR. In this case, neither the MCN nor MCFLMS algorithms succeeded, and a 0-dB NRMSPM was observed for SNRs up to 50 dB. Only the proposed NMCFLMS method can determine the channel impulse responses with reasonable accuracy. Fig. 10 shows its performance computed from 200-run Monte Carlo trials. At 50 dB SNR, the trajectories of the cost function $J(n)$ and the normalized misalignment $||\epsilon(n)||/||\mathbf{h}||$ for one typical run of the NMCFLMS algorithm are presented in Fig. 11. In addition, a comparison of impulse responses between the actual channels and their estimates is made in Fig. 12. Apparently, the NMCFLMS is more sensitive to noise while working on this system than on the previous one, but on the other hand, when the SNR is high, the misalignment decreases monotonically, and the time sequences of the estimated channel impulse responses are satisfactorily close to the actual ones.

## VI. Conclusion

The problem of blind multichannel identification and estimation was studied in the frequency domain. We addressed the issues of convergence, adaptivity, and efficiency of a satisfactory blind channel identification algorithm from a practical point of view. We reviewed the second-order statistics batch methods and pointed out that their inability to adapt is a critical drawback, particularly for real-time applications. By analyzing the performance of the time-domain adaptive approaches, we realized that they either converge slowly (e.g., the multichannel LMS algorithm) or involve extensive computation (e.g., the multichannel Newton algorithm). Aiming to resolve this dilemma and achieve a balance between fast convergence and low complexity, we proposed to implement the adaptive blind channel identification algorithms in the frequency domain.

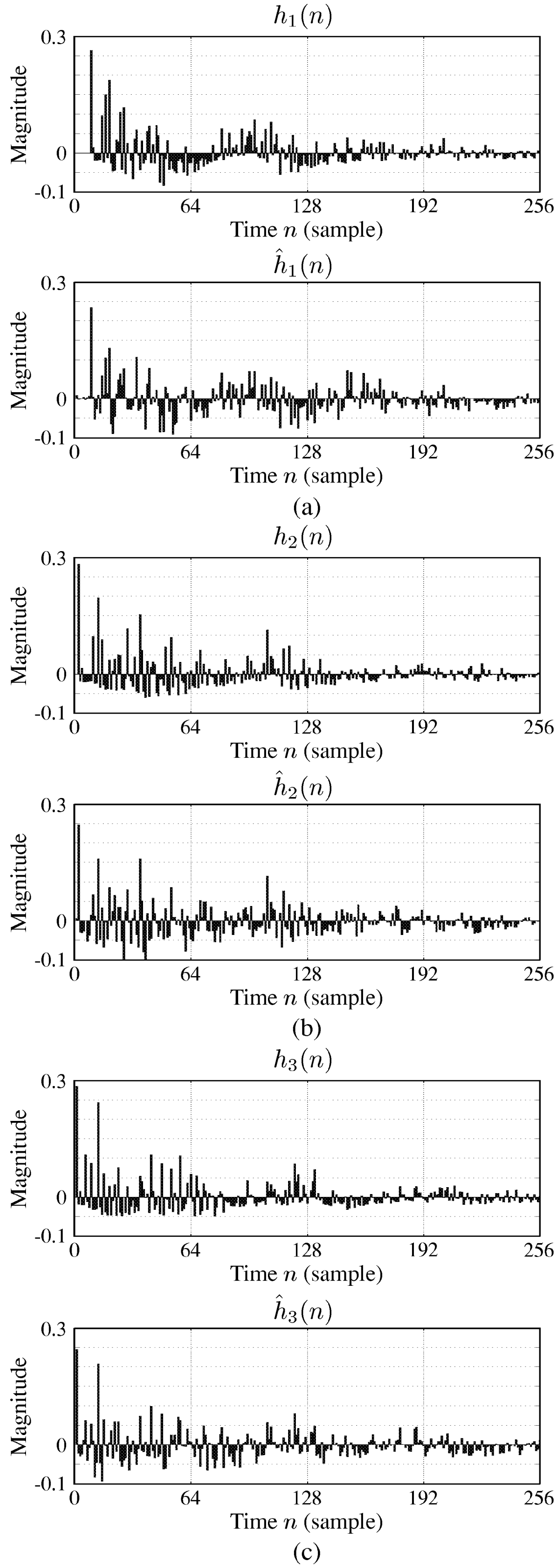


Fig. 12. Comparison of impulse responses between the actual channels and their estimates determined by using the NMCFLMS algorithm. The system is excited by the male speech signal of Fig. 6 at 50 dB SNR. (a) Channel 1. (b) Channel 2. (c) Channel 3.

By utilizing the overlap-save technique, a block error signal based on the cross relation between different channel outputs was established, and then, the multichannel frequency-domain LMS (MCFLMS) algorithm was derived to determine the desired channel estimate that minimizes the mean of the block error signal power. Since the time-domain convolutions and correlations are transformed to instantaneous multiplications through FFTs, the proposed MCFLMS is more computationally efficient. Further, in the spirit of Newton's method, the updates of the the adaptive filter coefficients in the frequency domain were normalized to make the filter coefficients converge independently and uniformly. The normalized multichannel frequency-domain LMS (NMCFLMS) algorithm was thereafter deduced. With a careful analysis, some approximations were made, and the normalization matrix became diagonal and was easy to invert. Therefore, we conclude that the NMCFLMS algorithm achieves both fast convergence and great efficiency. Extensive numerical studies were conducted. Many different multichannel systems with impulse responses of various lengths excited by either a BPSK sequence or a male speech signal were designed to evaluate the performance of the proposed algorithms. The results supported the appealing features we claimed for the proposed frequency-domain approaches. It is remarkable that for the three-channel acoustic system with long impulse responses (256 taps in each channel) excited by a male speech signal, only the proposed NMCFLMS algorithm succeeded in determining a reasonably accurate channel estimate. This observation lets the NMCFLMS algorithm find promising applications such as time delay estimation in speech processing.

## Acknowledgment

The authors would like to thank D. R. Morgan for carefully reading a draft and providing many constructive comments and suggestions that have improved the clarity of this paper.

## References

[1] Y. Sato, "A method of self-recovering equalization for multilevel amplitude-modulation," *IEEE Trans. Commun.*, vol. COM-23, pp. 679–682, June 1975.
[2] L. Tong, G. Xu, and T. Kailath, "A new approach to blind identification and equalization of multipath channels," in *Proc. 25th Asilomar Conf. Signals, Syst., Comput.*, vol. 2, 1991, pp. 856–860.
[3] E. Moulines, P. Duhamel, J. F. Cardoso, and S. Mayrargue, "Subspace methods for the blind identification of multichannel FIR filters," *IEEE Trans. Signal Processing*, vol. 43, pp. 516–525, Feb. 1995.
[4] H. Liu, G. Xu, and L. Tong, "A deterministic approach to blind equalization," in *Proc. 27th Asilomar Conf. Signals, Syst., Comput.*, vol. 1, 1993, pp. 751–755.
[5] G. Xu, H. Liu, L. Tong, and T. Kailath, "A least-squares approach to blind channel identification," *IEEE Trans. Signal Processing*, vol. 43, pp. 2982–2993, Dec. 1995.
[6] C. Avendano, J. Benesty, and D. R. Morgan, "A least squares component normalization approach to blind channel identification," in *Proc. IEEE Int. Conf. Acoust., Speech, Signal Process.*, vol. 4, 1999, pp. 1797–1800.
[7] D. Slock, "Blind fractionally-spaced equalization, prefect reconstruction filerbanks, and multilinear prediction," in *Proc. IEEE Int. Conf. Acoust., Speech, Signal Process.*, vol. 4, 1994, pp. 585–588.
[8] Y. Hua, "Fast maximum likelihood for blind identification of multiple FIR channels," *IEEE Trans. Signal Processing*, vol. 44, pp. 661–672, Mar. 1996.
[9] L. Tong and S. Perreau, "Multichannel blind identification: From subspace to maximum likelihood methods," *Proc. IEEE*, vol. 86, no. 10, pp. 1951–1968, Oct. 1998.
[10] Q. Zhao and L. Tong, "Adaptive blind channel estimation by least squares smoothing," *IEEE Trans. Signal Processing*, vol. 47, pp. 3000–3012, Nov. 1999.

[11] Y. Huang, J. Benesty, and G. W. Elko, "Adaptive eigenvalue decomposition algorithm for real-time acoustic source localization system," in *Proc. IEEE Int. Conf. Acoust., Speech, Signal Process.*, vol. 2, 1999, pp. 937–940.

[12] K. Berberidis, A. Marava, P. Karaivazoglou, and J. Palicot, "Robust and fast converging decision feedback equalizer based on a new adaptive semi-blind channel estimation algorithm," in *Proc. IEEE GLOBECOM*, vol. 1, 2001, pp. 269–273.

[13] Y. Huang and J. Benesty, "Adaptive multi-channel least mean square and Newton algorithms for blind channel identification," *Signal Process.*, vol. 82, pp. 1127–1138, Aug. 2002.

[14] M. Dentino, J. McCool, and B. Widrow, "Adaptive filtering in the frequency domain," *Proc. IEEE*, vol. 66, no. 12, pp. 1658–1659, Dec. 1978.

[15] J. B. Allen and D. A. Berkley, "Image method for efficiently simulating small-room acoustics," *J. Acoust. Soc. Amer.*, vol. 65, no. 4, pp. 943–950, Apr. 1979.

[16] A. V. Oppenheim and R. W. Schafer, *Discrete-Time Signal Processing*. Englewood Cliffs, NJ: Prentice-Hall, 1989.

[17] D. H. Brandwood, "A complex gradient operator and its application in adaptive array theory," *Proc. Inst. Elect. Eng. F, H*, vol. 130, pp. 11–16, Feb. 1983.

[18] S. Haykin, *Adaptive Filter Theory*. Englewood Cliffs, NJ: Prentice-Hall, 1996.

[19] J. Benesty and D. Morgan, "Frequency-domain adaptive filtering revisited, generalization to the multi-channel case, and application to acoustic echo cancellation," in *Proc. IEEE Int. Conf. Acoust., Speech, Signal Process.*, vol. 2, 2000, pp. 789–792.

[20] D. R. Morgan, J. Benesty, and M. M. Sondhi, "On the evaluation of estimated impulse responses," *IEEE Signal Processing Lett.*, vol. 5, pp. 174–176, July 1998.


**Yiteng (Arden) Huang** (M'01) received the B.S. degree from the Tsinghua University, Beijing, China, in 1994 and the M.S. and Ph.D. degrees from the Georgia Institute of Technology (Georgia Tech), Atlanta, in 1998 and 2001, respectively, all in electrical and computer engineering.

During his doctoral studies from 1998 to 2001, he was a research assistant with the Center of Signal and Image Processing, Georgia Tech, where he was also a teaching assistant with the School of Electrical and Computer Engineering. In the summers from 1998 to 2000, he was with Bell Laboratories, Murray Hill, NJ, where he was engaged in research on passive acoustic source localization with microphone arrays. In March 2001, he joined Bell Laboratories as a Member of Technical Staff. He is a co-editor/co-author of the book *Adaptive Signal Processing: Applications to Real-World Problems* (Berlin, Germany: Springer-Verlag, 2003). His current research interests are in adaptive filtering, multichannel signal processing, source localization, microphone array for hands-free telecommunication, speech enhancement, and statistical signal processing.

Dr. Huang is currently an associate editor of the IEEE SIGNAL PROCESSING LETTERS. He received the 1997–1998 Colonel Oscar P. Cleaver Outstanding Graduate Student Award from the School of Electrical and Computer Engineering, Georgia Tech, a 2000 Outstanding Research Award from the Center of Signal and Image Processing, Georgia Tech, and a 2000–2001 Outstanding Graduate Teaching Assistant Award from the School of Electrical and Computer Engineering, Georgia Tech.

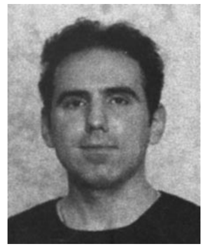

**Jacob Benesty** (M'92) was born in Marrakech, Morocco, in 1963. He received the Masters degree in microwaves from Pierre and Marie Curie University, Paris, France, in 1987 and the Ph.D. degree in control and signal processing from Orsay University, Orsay, France, in April 1991.

During his Ph.D. program (from November 1989 to April 1991), he worked on adaptive filters and fast algorithms at the Centre National d'Etudes des Telecommunications (CNET), Paris. From January 1994 to July 1995, he was with Telecom Paris, where he worked on multichannel adaptive filters and acoustic echo cancellation. He joined Bell Labs, Lucent Technologies (formerly AT&T), Murray Hill, NJ, in October 1995, first as a Consultant and then as a Member of Technical Staff. He has since been working on stereophonic acoustic echo cancellation, adaptive filters, source localization, robust network echo cancellation, and blind deconvolution. He co-authored the book *Advances in Network and Acoustic Echo Cancellation* (Berlin: Springer-Verlag, 2001). He is also a co-editor/co-author of the books *Adaptive Signal Processing: Applications to Real-World Problems* (Berlin, Germany: Springer-Verlag, 2003) and *Acoustic Signal Processing for Telecommunication* (Boston, MA: Kluwer, 2000).

Dr. Benesty received the 2001 best paper award from the IEEE Signal Processing Society. He was the co-chair of the 1999 International Workshop on Acoustic Echo and Noise Control.